Cardiovascular Research (2015) **106**, 143–152
doi:10.1093/cvr/cvu262

Neuronal Na^+ channel blockade suppresses arrhythmogenic diastolic Ca^{2+} release

Przemysław B. Radwański[1,2,3]*, Lucia Brunello[1,2], Rengasayee Veeraraghavan[4], Hsiang-Ting Ho[1,2], Qing Lou[1,2], Michael A. Makara[1,2], Andriy E. Belevych[1,2], Mircea Anghelescu[5], Silvia G. Priori[6], Pompeo Volpe[7], Thomas J. Hund[1], Paul M. L. Janssen[1,2], Peter J. Mohler[1,2,8], John H. B. Bridge[9], Steven Poelzing[4], and Sándor Györke[1,2]*

[1]Dorothy M. Davis Heart and Lung Research Institute, College of Medicine, The Ohio State University Wexner Medical Center, 473 West 12th Avenue, Room 507, Columbus, OH 43210, USA; [2]Department of Physiology and Cell Biology, College of Medicine, The Ohio State University, Columbus, OH, USA; [3]Division of Pharmacy Practice and Administration, College of Pharmacy, The Ohio State University, Columbus, OH, USA; [4]VTC Research Institute, School of Biomedical Engineering and Sciences, Virginia Tech, Roanoke, VA, USA; [5]Department of Biological and Allied Health Sciences, Ohio Northern University, Ada, OH, USA; [6]Division of Cardiology and Molecular Cardiology, Maugeri Foundation–University of Pavia, Pavia, Italy; [7]Department of Biomedical Sciences, University of Padova, Padova, Italy; [8]Department of Internal Medicine, College of Medicine, The Ohio State University, Columbus, OH, USA; and [9]Nora Eccles Harrison Cardiovascular Research and Training Institute, University of Utah, Salt Lake City, UT, USA

Received 22 May 2014; revised 26 November 2014; accepted 4 December 2014; online publish-ahead-of-print 23 December 2014

Time for primary review: 39 days

Aims Sudden death resulting from cardiac arrhythmias is the most common consequence of cardiac disease. Certain arrhythmias caused by abnormal impulse formation including catecholaminergic polymorphic ventricular tachycardia (CPVT) are associated with delayed afterdepolarizations resulting from diastolic Ca^{2+} release (DCR) from the sarcoplasmic reticulum (SR). Despite high response of CPVT to agents directly affecting Ca^{2+} cycling, the incidence of refractory cases is still significant. Surprisingly, these patients often respond to treatment with Na^+ channel blockers. However, the relationship between Na^+ influx and disturbances in Ca^{2+} handling immediately preceding arrhythmias in CPVT remains poorly understood and is the object of this study.

Methods and results We performed optical Ca^{2+} and membrane potential imaging in ventricular myocytes and intact cardiac muscles as well as surface ECGs on a CPVT mouse model with a mutation in cardiac calsequestrin. We demonstrate that a subpopulation of Na^+ channels (neuronal Na^+ channels; nNa_v) colocalize with ryanodine receptor Ca^{2+} release channels (RyR2). Disruption of the crosstalk between nNa_v and RyR2 by nNa_v blockade with riluzole reduced and also desynchronized DCR in isolated cardiomyocytes and in intact cardiac tissue. Such desynchronization of DCR on cellular and tissue level translated into decreased arrhythmias in CPVT mice.

Conclusions Thus, our study offers the first evidence that nNa_v contribute to arrhythmogenic DCR, thereby providing a conceptual basis for mechanism-based antiarrhythmic therapy.

Keywords Ventricular arrhythmias • Neuronal Na^+ channels • Diastolic Ca^{2+} release

1. Introduction

Sudden arrhythmic death is a leading cause of mortality in the USA.[1] Arrhythmias caused by abnormal impulse generation occur both in patients with structural heart disease,[2] as well as in seemingly healthy individuals.[3] In the latter, fatal arrhythmias are often associated with aberrant diastolic Ca^{2+} release (DCR) during exercise or stress-induced catecholamine surge.[3] These are called Catecholaminergic Polymorphic Ventricular Tachycardia (CPVT).[4] Recent evidence suggests that CPVT is related to mutations in proteins comprising the ryanodine receptor Ca^{2+} release channel (RyR2) complex, including the RyR2 itself and the sarcoplasmic reticulum (SR) Ca^{2+}-binding protein calsequestrin (CASQ2).[5,6] These mutations appear to alter the ability of RyR2 to become refractory following systolic Ca^{2+} release, allowing it to remain open during diastole and leak SR Ca^{2+}.[7–10] This can result in DCR, which in turn can be translated into membrane depolarization via electrogenic Na^+/Ca^{2+} exchange (NCX) resulting in triggered ventricular arrhythmia.[8,10–12]

* Corresponding author. Tel: +614 292 3969; fax: +614 247 7799, Email: sandor.gyorke@osumc.edu (S.G.); Tel: +614 292 3944; fax: +614 247 7799, Email: przemyslaw.radwanski@osumc.edu (P.B.R.)

Despite high response of CPVT to combination of Ca^{2+} channel- and β-blockers, the incidence of refractory cases is still significant.[13] Surprisingly, based on the Ca^{2+}-dependent mechanisms, such patients often respond to treatment with Na^+ channel blockade.[13] However, the precise contribution of Na^+ influx to aberrant DCR and arrhythmogenesis is unclear. Data presented herein strongly suggest that a subpopulation of Na^+ channels, neuronal Na^+ channels (nNa_v), colocalize with RyR2. The electrogenic NCX couples Na^+ fluxes in these compartments to Ca^{2+} influx and efflux as well as membrane potential. Disruption of coupling between nNa_v and RyR2 by nNa_v blockade reduced and desynchronized DCR in isolated cardiomyocytes as well as in tissue and decreased arrhythmias in CPVT mice. Thus, our study offers the first support for the concept that nNa_v contribute to the genesis and synchronization of arrhythmogenic DCR and identifies nNa_v as a target for mechanism-based antiarrhythmic therapy.

2. Methods

All animal procedures were approved by The Ohio State University Institutional Animal Care and Use Committee and conformed to the Guide for the Care and Use of Laboratory Animals published by the US National Institutes of Health (NIH Publication No. 85-23, revised 2011).

2.1 Myocyte isolation, confocal Ca^{2+} imaging, Na^+ current, and membrane potential recordings

Ventricular myocytes were obtained by enzymatic isolation from 3- to 5-month-old R33Q (in C57BL/6 background) and age-matched C57BL/6 WT (Jackson Jax Lab) male mice. Mice were anaesthetized with isoflurane, and once a deep level of anaesthesia was reached, confirmed by lack of response to noxious stimuli, the heart was rapidly removed and perfused via a Langendorff as previously described.[8] Single ventricular myocytes were isolated using Liberase Blendzymes (Roche, Applied Science, IN, USA). Whole-cell patch clamp recordings of action potentials were performed with an Axopatch 200B amplifier using external solution that contained (in mM): 140 NaCl, 5.4 KCl, 2.0 $CaCl_2$, 0.5 $MgCl_2$, 10 HEPES, and 5.6 glucose (pH 7.4). Patch pipettes were filled with a solution that contained (in mM): 90 K-aspartate, 50 KCl, 5 MgATP, 5 NaCl, 1 $MgCl_2$, 0.1 Tris GTP, 10 HEPES, and 0.1 Fluo-4 K-salt (Molecular Probes, Eugene, OR, USA) (pH 7.2). Sodium currents (I_{Na}) were recorded using internal solution containing (in mM): 10 NaCl, 20 TEACl, 123 CsCl, 1 $MgCl_2$, 0.1 Tris GTP, 5 MgATP, 10 HEPES, and 10 BAPTA (pH 7.2). The extracellular bathing solution contained (in mM): 10 NaCl, 130 TEACl, 4 CsCl, 0.4 $CaCl_2$, 2 $MgCl_2$, 0.05 $CdCl_2$, 10 HEPES, and 10 glucose; pH was maintained at 7.4 with CsOH. Whole-cell capacitance and series resistance compensation (≥60%) was applied along with leak subtraction. Electrical field stimulation experiments were performed using the following external solution (in mM): 140 NaCl, 5.4 KCl, 2.0 $CaCl_2$, 0.5 $MgCl_2$, 10 HEPES, and 5.6 glucose (pH 7.4). For Ca^{2+} spark recordings in permeabilized myocytes, the cardiac myocytes were permeabilized with saponin (0.01% for 20–30 s). The internal solution contained (in mM): 120 K-aspartate, 20 KCl, 0.81 $MgCl_2$, 1 KH_2PO_4, 0.5 EGTA (free [Ca^{2+}] ~50 nm), 3 MgATP, 10 phosphocreatine, 0.03 Fluo-4 K-salt, 20 HEPES (pH 7.2), and 5 U/mL creatine phosphokinase. To assess the SR Ca^{2+} load, 20 mM caffeine was applied at the end of the experiments. Intracellular Ca^{2+} cycling was monitored by a Nikon A1 laser scanning confocal microscope equipped with a ×60 1.4 NA oil objective. For intact myocytes, we used the cytosolic Ca^{2+}-sensitive indicators Fluo-4 AM (Ca^{2+} sparks) and Fluo-4FF AM (Ca^{2+} waves). The fluorescent probes were excited with the 488 nm line of an argon laser, and emission was collected at 500–600 nm. Fluo-4/Fluo-4FF fluorescence was recorded in the line scan mode of the confocal microscope (0.207 μm per pixel, 1–5 ms per line). For Ca^{2+} wave recordings, myocytes were paced at 0.3 Hz using extracellular platinum electrodes to obtain a comprehensive distribution of the first DCR latencies. Any DCR event (i.e. wave, wavelet) that increased cell-wide fluorescence intensity above 10% of the signal generated by the preceding stimulated Ca^{2+} transient was included in the analysis. The fluorescence emitted was expressed as F/F_0, where F is the fluorescence at time t and F_0 represents the background signal. All experiments were performed at room temperature (26°C).

2.2 Cardiac muscles confocal Ca^{2+} and membrane potential imaging

Muscles for confocal Ca^{2+} and membrane potential imaging were prepared as previously described.[8] Briefly, the hearts were removed and placed in a modified Krebs–Henseleit (KH) buffer, containing (in mmol/L) 120 NaCl, 5 KCl, $2MgSO_4$, 1.2 NaH_2PO_4, 20 $NaHCO_3$, 0.25 $CaCl_2$, and 10 glucose (pH 7.4), equilibrated with 95% O_2–5% CO_2. Twenty millimolar 2,3-butanedione monoxime (BDM) was also added to the dissection buffer to minimize cutting injury. The recording chamber was placed on the stage of an Olympus FluoView 1000 laser scanning confocal microscope, equipped with a 5 mW He–Ne laser and a UPLSAPO 60X water objective (NA 1.20, working distance 0.28 mm). Muscles were loaded with the cytosolic Ca^{2+} indicator Rhod-2 AM for 45 min and di-4-ANBDQBS (Richard D. Berlin Center for Cell Analysis and Modeling, University of Connecticut Health Center, USA) for 10 min. The muscles were superfused with KH buffer containing 5 mM BDM and 10–20 μM blebbistatin to stop cell contraction. The Ca^{2+} concentration was also raised in the KH buffer to 1.5 mM. Line-scan images were acquired at the rate of 8 μs/pixel. The fluorescence emitted was expressed as F/F_0, where F is the fluorescence at time t and F_0 represents the background signal. All experiments were performed at room temperature.

2.3 Confocal microscopy of immunolabelled myocytes and image analysis

Isolated ventricular myocytes from R33Q hearts were plated on laminin-coated glass coverslips, fixed with 4% paraformaldehyde (5 min), permeabilized with 0.1% Triton X-100, and washed with PBS. Endogenous immunoglobulin was blocked using a mouse-on-mouse blocking reagent (M.O.M. kit; Vector Laboratories, Burlingame, CA, USA) for 1 h at room temperature and subsequently incubated with primary antibodies overnight at 4°C. After washing, goat secondary antibodies (anti-mouse and anti-rabbit) conjugated to Alexa Fluor (488, 594; Life Technologies, Grand Island, NY, USA) were added for 1 h. Coverslips were mounted to using ProLong Gold Anti-Fade Mounting Kit (Molecular Probes).

Immunolabelled myocytes were imaged on a TCS SP8 laser scanning confocal microscope equipped with a ×63/1.4 numerical aperture oil objective (Leica, Buffalo Grove, IL, USA). Custom software written in Matlab (Mathworks, Natick, MA) was used to analyse images for colocalization and cross-correlation as well as to perform fast Fourier transform (FFT) morphological analysis. Briefly, colocalization was assessed from plots of red vs. green intensity as previously described.[14] Additionally, the cross-correlation coefficient between the intensities of red and green immunofluorescent signals was calculated both row-wise as well as for the averaged intensity profile over a whole myocyte. Further morphological analysis was performed by calculating the two-dimensional (2D) FFT for the red and green channels of each image. The amplitude of the 2D FFT for the red and green channels, each itself in the form of a 2D image with the same dimensions as the original image, was then overlaid. Periodicity of immunofluorescent signal was assessed from the location and amplitude of peaks on the FFTs and the relative periodicities of the red and green immunofluorescent signals assessed from the overlaid FFTs of the respective channels. The antibodies used were rabbit anti-$Na_V1.1$, 1.3, 1.6 (Alomone, Jerusalem, Israel), 1.5 (generous gift from Dr Peter Mohler), and mouse monoclonal anti-RyR2 (Pierce Antibodies, Rockford, IL, USA).

2.4 ECG recordings

ECG recordings were performed before and after epinephrine and caffeine challenge. Continuous ECG recordings were obtained from mice anaesthetized with isoflurane, at minimum effective concentration (1–1.5%). Subcutaneous needle electrodes were applied to the left, right upper limb, and right lower limb for ECG recording (PL3504 PowerLab 4/35, ADInstruments). After baseline recording (5 min.), each mouse received intraperitoneally vehicle (DMSO), riluzole (10 mg/kg), or SN-6 (40 mg/kg). After 5–10 min from the initial intervention, animals were exposed to an intraperitoneally epinephrine (Epi, 1.5 mg/kg) and caffeine (Caff, 120 mg/kg) challenge, and ECG recording continued for 10 min. ECG recordings were analysed using the LabChart 7.3 program (ADInstruments). Ventricular tachycardia (VT) was defined as three or more premature ectopies, while arrhythmia was defined as frequent ectopies, bigeminies, and/or VT.

2.5 Reagents

Unless otherwise stated, all chemicals were purchased from Sigma (St Louis, MO, USA), Torcis (Bristol, UK), or Alomone. Fluorescent dyes were purchased from either Molecular Probes or Richard D. Berlin Center for Cell Analysis and Modeling (University of Connecticut Health Center, USA).

2.6 Data analysis

Membrane potential and I_{Na} analysis were performed using pCLAMP9 software (Molecular Devices, Sunnyvale, CA, USA). Line scanning images of Ca^{2+} and membrane potential were normalized for baseline fluorescence.[8] Ca^{2+} and membrane potential imaging data were processed using ImageJ and Origin software. Statistical analysis of the data was performed using a two-tailed Student's *t*-test for paired and unpaired data or a single factor ANOVA. The Šidák correction was applied to adjust for multiple comparisons. A Fisher's exact and a Mantel–Haenszel test were used to test differences in nominal data. All values are reported as means ± SEM unless otherwise noted. A value of $P < 0.05$ was considered statistically significant.

3. Results

3.1 Neuronal Na^+ channel modulation regulates DCR

To determine whether nNa_v possess a unique action on intracellular Ca^{2+} handling that may serve as a substrate for triggered arrhythmias, we assessed the impact of nNa_v blockade on Ca^{2+} sparks and DCR in the form of Ca^{2+} waves in cardiomyocytes isolated from hearts expressing a CPVT-associated CASQ2 mutation (R33Q) and exposed to isoproterenol (Iso).[15] In accord with previous observations,[16] R33Q cardiomyocytes evidenced a high rate of SR Ca^{2+} leak that corresponded to high Ca^{2+} spark frequency and prolonged duration of release. Tetrodotoxin (TTX) at nanomolar concentration is known to selectively inhibit nNa_v without significantly affecting cardiac-type Na^+ channels ($Na_v1.5$) or directly inhibiting RyR2.[17–20] Line-scan confocal Ca^{2+} imaging showed that 100 nM TTX significantly decreased the frequency of Iso-promoted Ca^{2+} sparks and DCR in resting and paced cardiomyocytes, respectively (*Figure 1A–E*). We also assessed DCR synchrony, a marker of Ca^{2+} release refractoriness.[8,10] TTX significantly reduced DCR synchrony, as demonstrated by a broadened distribution of DCR first latencies and an increase in the S.D. of latency (*Figure 1F*). Notably, TTX's antiarrhythmic effects were not accompanied by alterations in the SR Ca^{2+} content or Ca^{2+} transient amplitude (see Supplementary material online, *Figure S1A–C*), which is consistent with a previous report that utilized TTX concentrations of up to 5 μM.[21] The sensitivity of DCR in R33Q ventricular cardiomyocytes to 100 nM TTX might have resulted from an adaptive up-regulation of nNa_v. To address such possibility, we assessed peak Na^+ current (I_{Na}) in R33Q and WT myocytes. There was no significant difference in I_{Na} density between the two study cohorts (*Figure 2A* and *B*).

Next, we investigated the antiarrhythmic effects of nNa_v inhibition using riluzole,[22] an agent with an established clinical efficacy in management of amyotrophic lateral sclerosis (ALS).[23] First, we assessed whether riluzole inhibits the TTX-sensitive component of I_{Na}. To this end, we compared I_{Na} reduction between 100 nM TTX and 10 μM riluzole. In WT cardiomyocytes, we observed no significant difference in the reduction of peak I_{Na} (32.5 ± 7.7 vs. 35.1 ± 4.2%) between the two pharmacological interventions (*Figure 2C*). Furthermore, both riluzole and TTX facilitated I_{Na} inactivation as evidenced by a reduction in the slow component of the decaying phase of I_{Na} (*Figure 2D* and *E*). Importantly, effects of 10 μM riluzole on excitability (Supplementary material online, *Figure S2A* and *B*), Ca^{2+} release (*Figure 1A–E*; Supplementary material online, *Figure S1A–C*), and Ca^{2+} release synchrony (*Figure 1E*) were similar to those observed with TTX.[20,24] Lastly, riluzole did not affect Ca^{2+} spark frequency in permeabilized cardiomyocytes (8.73 ± 0.49 vs. 7.69 ± 0.36 Sparks/100 μm/s, P = ns, n = 634–700 events), suggesting that riluzole lacks a direct effect on RyR2.

To assess whether modulation of nNa_v inactivation[25] (*Figure 2D* and *E*) can in part contribute to the generation of DCR in quiescent (non-stimulated) myocytes, we facilitated as well as slowed nNa_v inactivation with riluzole (10 μM) and β-pompilidotoxin (β-PMTX, 50 μM), respectively.[26] In catecholamine-free wild-type (WT) myocytes, we observed riluzole-mediated decrease in Ca^{2+} spark frequency (*Figure 3A–C*). On the other hand, β-PMTX increased frequency of Ca^{2+} sparks in WT myocytes despite the omission of catecholamines (*Figure 3A–C*). Furthermore, the enhanced Na^+ flux at rest translated into increased rate of DCR frequency in stimulated, catecholamine-exposed WT cardiomyocytes (*Figure 3D* and *E*). Additionally, such rise in DCR was coupled to abbreviated latency to the first DCR and reduced SR Ca^{2+} content (*Figure 3F*; Supplementary material online, *Figure S1E* and *F*). This reduction in SR Ca^{2+} content can perhaps be ascribed to a large reverse mode NCX (Na^+-out and Ca^{2+}-in) in the junctional cleft prompted by enhanced Na^+ influx via the incompletely inactivated nNa_v. Of note, the effects of β-PMTX on Ca^{2+} cycling were reversed with riluzole (*Figure 3A–E*; Supplementary material online, *Figure S1D–F*). Importantly, the effects of nNa_v modulation were independent of global phosphorylation state of the cardiomyocyte. Neither Ca^{2+}/calmodulin-dependent protein kinase II inhibition with KN-93 (5 μM) in the presence of Iso nor the complete omission of Iso from the superfusate prevented nNa_v modulation of aberrant Ca^{2+} release (*Figure 3A–C*; Supplementary material online, *Figure S2C* and *D*). Taken together these results strongly suggest that a specific subpopulation of Na^+ channels (i.e. nNa_v) exert a modulatory effect on DCR, which likely involves NCX.

To assess the role of NCX in the interaction between nNa_v and RyR2, we inhibited reverse mode NCX (Na^+-out and Ca^{2+}-in) with SN6 (5 μM).[27,28] Effects on DCR similar to those observed with nNa_v blockade were obtained with SN6 (*Figures 1* and *3*; Supplementary material online, *Figure S1*). Furthermore, no significant effect was observed on forward mode NCX (Ca^{2+}-out and Na^+-in) as assessed by the decay of the caffeine-induced Ca^{2+} transient (Supplementary material online, *Figure S1C*, inset). These data suggest that NCX can regulate Ca^{2+} release[29] and is an integral part of the pro-arrhythmic interaction between nNa_v and RyR2 within R33Q cardiomyocytes.

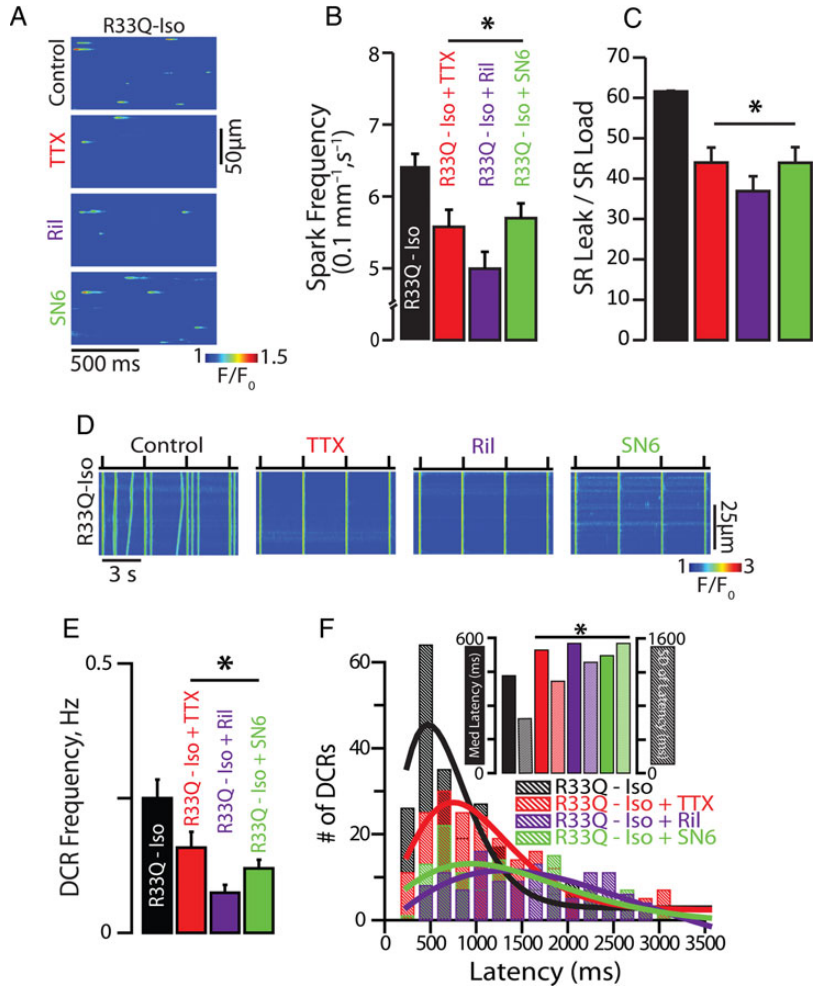

Figure 1 Neuronal Na^+ channel blockade disrupts Na^+/Ca^{2+} signalling and suppresses DCR. (*A*) Representative examples of the line-scan images of Ca^{2+} sparks recorded in R33Q ventricular cardiomyocytes. Cells were treated with TTX (100 nM), riluzole (Ril, 10 μM), and SN6 (5 μM) (*B*) TTX ($n = 1054$ events from 47 cells isolated from four mice), Ril ($n = 1675$ events from 59 cells isolated from three mice), and SN6 ($n = 2811$ events from 84 cells isolated from three mice) significantly decreased Ca^{2+} spark frequency in Iso-treated R33Q myocytes ($n = 2442$ events from 90 cells isolated from seven mice) (*C*) resulting in a reduction of SR Ca^{2+} load normalized spark-mediated SR Ca^{2+} leak (=spark mass × spark frequency/SR Ca^{2+} content) ($n = 38$, 19, 22, and cells isolated from 3–4 mice for TTX, Ril, and SN6, respectively) compared with Iso alone ($n = 41$ cells isolated from seven mice, $^*P < 0.05$). (*D*) Representative examples of the line-scan images of Iso-stimulated R33Q and WT ventricular cardiomyocytes paced at 0.3 Hz. (*E*) TTX ($n = 66$ cells from four mice), Ril ($n = 67$ cells from two mice), and SN6 ($n = 50$ cells from three mice) significantly decreased DCR events in the form of Ca^{2+} waves in Iso-treated R33Q myocytes ($n = 93$ cells isolated from eight mice), (*F*) delayed the latency to the first DCR, as well as reduced DCR synchronicity as demonstrated by a broadened distribution of DCR first latencies and (inset) an increase in the median latency and S.D. of the latency compared with Iso alone (TTX, $n = 208$ events; Ril, $n = 118$ events; SN6, $n = 129$ events vs. Iso alone, $n = 237$ events, $^*P < 0.05$).

3.2 Neuronal Na^+ channels and RyR2 colocalize

Experiments in isolated myocytes suggest that localization of nNa_v in close proximity to SR Ca^{2+}-release machinery is consistent with their role in precipitating DCR. Therefore, we performed confocal immunolocalization experiments in ventricular myocytes isolated from R33Q hearts. Over 80% of the nNa_v ($Na_v1.1$, 1.3, 1.6) immunofluorescent signal coincided with RyR2 labelling (*Figure 4A–C* and *E–G*) and exhibited a periodic pattern consistent with T-tubular localization (Supplementary material online, *Figure S3A–C*, *E–G*, *S4*, and *S5A*).[30,31] On the other hand, very little spatial cross-correlation was observed between regions labelled with cardiac-type Na^+ channels ($Na_v1.5$) and RyR2 (*Figure 4D* and *H*; Supplementary material online, *Figure S3D*, *H*, and *S5B*). These results strongly suggest that nNa_v colocalize with RyR2 in the same subcellular regions in the R33Q mouse ventricle and in part may explain nNa_v contribution to the regulation of DCR in a setting of leaky RyR2.

3.3 Neuronal Na^+ channel blockade desynchronizes DCR in tissue

We examined the role of nNa_v in DCR and focal excitation in tissue. We hypothesized that in a setting of leaky RyR2,[32,33] nNa_v could facilitate temporal alignment or synchronization of DCRs, and the resultant membrane depolarization in neighbouring cells accounting for the generation of ventricular extrasystole across the myocardium. Therefore, we performed simultaneous confocal imaging of membrane potential and

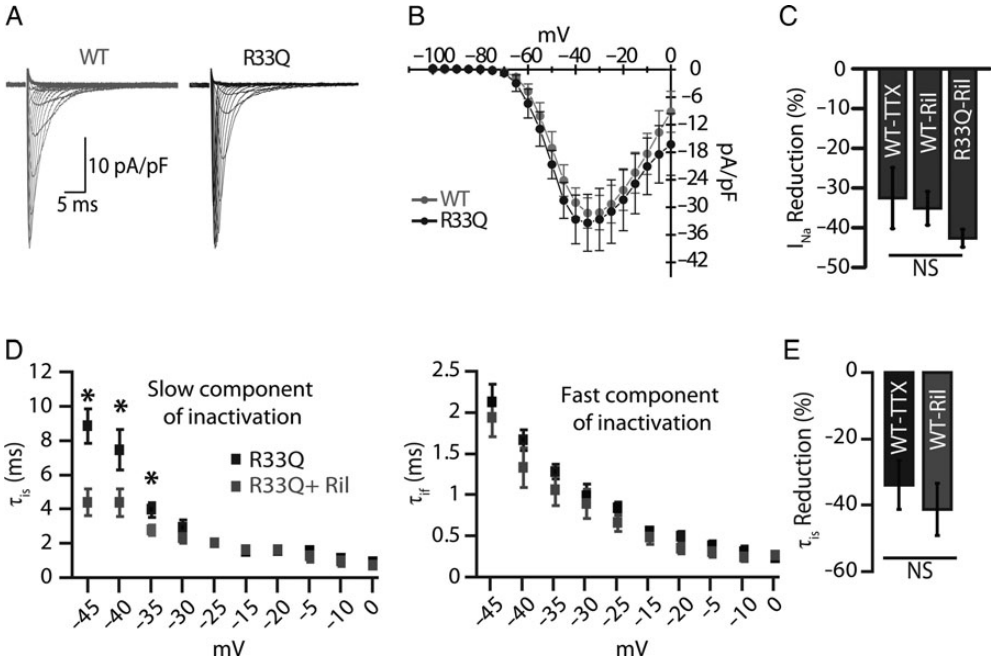

Figure 2 Effect of neuronal Na^+ channel blockade with riluzole on peak Na^+ current. (*A*) Inward Na^+ currents obtained by 250 ms depolarization steps from holding potential −120 to 0 mV in 5 mV increments at 3 s intervals. (*B*) Corresponding peak *I/V* relationship ($n = 9$ cells from five mice for WT and $n = 6$ cells from two mice for R33Q). (*C*) Reduction of Na^+ current by 100 nM TTX and 10 μM Ril ($n = 5$ cells from two mice for TTX, $n = 7$ cells from two mice for Ril in WT, and $n = 4$ cells from two mice for Ril in R33Q, $^*P < 0.05$). (*D*) The decaying phase of Na^+ current traces was fitted to 2-exponential function yielding two time constants, one slow (τ_{is}) and the other to fast component (τ_{if}). The effect of 10 μM Ril in R33Q cardiomyocytes ($n = 4$ cells from two mice, $^*P < 0.05$) on the decaying phase of Na^+ current with two components, slow (τ_{is}) and a fast (τ_{if}). (*E*) Reduction of the slow (τ_{is}) component of decaying phases of Na^+ current by 100 nM TTX and 10 μM Ril in WT cardiomyocytes ($n = 4$ cells from two mice and $n = 6$ cells from two mice, respectively, $^*P < 0.05$).

cytosolic Ca^{2+} in cardiac muscle preparations from R33Q mice during nNa_v blockade. Both riluzole (10 μM) and TTX (100 nM) significantly reduced frequency and synchronicity of Iso-promoted DCR (*Figure 5A–E*). Correspondingly, both drugs reduced the frequency of extrasystolic action potentials (*Figure 5E*). Thus, nNa_v blockade with riluzole can reduce DCR, its synchronicity, and the resultant triggered arrhythmias in cardiac muscle.

3.4 Effect of neuronal Na^+ channel blockade on CPVT

We next examined the therapeutic efficacy of disrupting the crosstalk between nNa_v and the leaky RyR2 on the cellular level that desynchronized DCR in intact tissue. To this end, we assessed arrhythmia inducibility in R33Q mice. A caffeine and epinephrine challenge induced frequent ventricular bigeminy (*Figure 6A*), which degenerated into polymorphic VT. After riluzole treatment (10 mg/kg), half of the R33Q animals remained in sinus rhythm (*Figure 6B*) despite the caffeine and epinephrine challenge. Overall, riluzole reduced by half ventricular arrhythmias, including frequent ventricular extrasystoles and bigeminies (*Figure 6D*), while completely suppressing VTs in all R33Q mice tested (*Figure 6E*). Consistent with observations in isolated cardiomyocytes, riluzole's antiarrhythmic effect in R33Q mice was modulated by perturbations of NCX-dependent Na^+/Ca^{2+} signalling. NCX inhibition with SN-6 (40 mg/kg, *Figure 6C–E*) resulted in a reduced overall arrhythmia burden. Taken together, these data suggest that perturbing local crosstalk between nNa_v and RyR2 via nNa_v blockade exerts an antiarrhythmic effect *in vivo* by reducing and desynchronizing DCR.

4. Discussion

Here we studied CPVT-associated arrhythmogenesis resulting from aberrant DCR.[15,35] Previous studies showed that CPVT-linked mutations disrupt RyR2 gating, thereby precipitating synchronous DCR and triggered arrhythmias.[5,8,36] In recent years, Na^+ channel blockade has emerged as a potential antiarrhythmic strategy in genetic and acquired models of Ca^{2+}-mediated arrhythmias.[13,19,21] Previous studies have suggested two mechanisms for the antiarrhythmic effect of Na^+ channel blockers such as flecainide: (i) direct inhibition of the RyR2[37] or (ii) decreased membrane excitability due to cardiac-type Na^+ channel ($Na_v1.5$) blockade uncoupling DCR from membrane depolarization.[38] Our results demonstrate a novel mechanism for Ca^{2+}-mediated arrhythmogenesis which involves Na^+/Ca^{2+} signalling independent of direct RyR2 block and reduced excitability. Importantly, disruption of the Na^+/Ca^{2+} signalling via inhibition of neuronal Na^+ channels (nNa_v) effectively suppressed arrhythmias in CPVT mice, thus suggesting a new therapeutic approach in management of CPVT.

Initially, the antiarrhythmic effect of Na^+ channel blockers, such as flecainide, was attributed to the direct inhibition of the RyR2.[37] Yet, riluzole did not reduce spark frequency in permeabilized myocytes in the present study arguing against its interacting directly with RyR2. Subsequent studies have suggested that decreased membrane excitability as

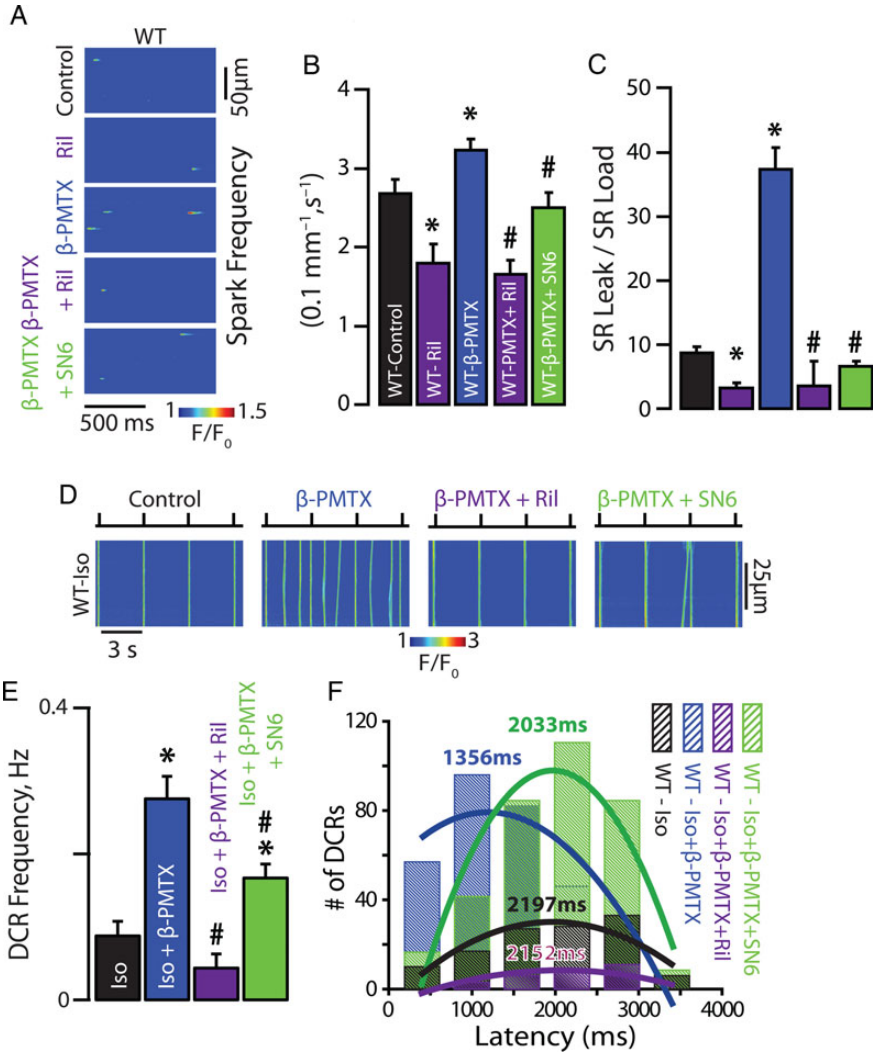

Figure 3 Neuronal Na^+ channel contribute to Na^+/Ca^{2+} signalling and DCR. (*A*) Representative examples of the line-scan images of Ca^{2+} sparks recorded in WT ventricular cardiomyocytes. nNa_v blockade with Ril in WT myocytes reduced Ca^{2+} spark frequency, while augmentation of the current passed by nNa_v with β-PMTX increased Ca^{2+} spark frequency. (*B*) Ril decreased ($n = 199$ events from 49 cells isolated from two mice) while β-PMTX increased Ca^{2+} spark frequency ($n = 2413$ events from 159 cells isolated from six mice) relative to catecholamine-free control ($n = 1363$ events from 115 cells isolated from eight mice). (*C*) Ril ($n = 27$ cells isolated from two mice) decreased while β-PMTX ($n = 36$ cells isolated from six mice) increased SR Ca^{2+} load normalized spark-mediated SR Ca^{2+} leak relative to catecholamine-free control ($n = 29$ cells isolated from eight mice, $^*P < 0.05$). Ril and SN6 significantly reversed the effects of β-PMTX on Ca^{2+} spark properties ($n = 293$ and 753 events from 51 and 65 cells isolated from three mice for Ca^{2+} spark, respectively, and $n = 27$ and 24 cells isolated from three mice for SR Ca^{2+} load normalized spark-mediated SR Ca^{2+} leak, respectively, $^{\#}P < 0.05$). (*D*) Representative examples of the line-scan images of Iso-stimulated WT ventricular cardiomyocytes paced at 0.3 Hz. (*E*) Augmentation of the current passed by nNa_v with β-PMTX in WT myocytes ($n = 95$ cells isolated from seven mice for β-PMTX and $n = 38$ cells isolated from five mice for Iso alone, $^*P < 0.05$) increased DCR frequency and (*F*) shortened the latency to the first DCR relative to Iso alone ($n = 309$ events for PMTX and $n = 121$ for Iso alone, $^*P < 0.05$). Ril and SN6 significantly reversed the effects of β-PMTX on DCR frequency ($n = 30$ and 86 cells isolated from three mice, respectively, $^{\#}P < 0.05$, $^*P < 0.05$ vs. Iso alone) and latency ($n = 97$ and 343 events, respectively).

a result of Na^+ channel blockade uncouples DCR from membrane depolarization.[38] However, neither 10 μM riluzole in our study nor 100 nM TTX in previous ones altered membrane excitability.[19,20,39] Importantly, our findings point to a distinct microdomain where nNa_v are localized near RyR2s (*Figure 4*), forming the functional unit underlying arrhythmogenic DCR in CPVT (*Figure 6F*). This is in accord with previous studies that have demonstrated the presence of nNa_v in the T-tubule.[31,40–43] We further demonstrate using pharmacological modulation of nNa_v (i.e. inhibition with TTX and riluzole and augmentation with β-PMTX) as well as NCX activity (SN6) that the unique interplay between Na^+ and Ca^{2+} handling within this domain is key to the pro-arrhythmic process. More precisely, in CPVT where cardiomyocytes exhibit increased baseline pro-arrhythmic RyR2 Ca^{2+} leak, nNa_v, and NCX blockade reduced DCR and suppressed arrhythmic activity on cellular level (*Figures 1* and *3*) and in tissue isolated from CPVT hearts (*Figure 5*). The results of these functional experiments taken together with colocalization of nNa_v (but not cardiac isoform of Na^+ channel) with RyR2 make a very compelling case for the involvement of nNa_v in the modulation of the arrhythmic DCR. However, this does not preclude the cardiac isoform of the Na^+ channel from participating in the arrhythmogenic

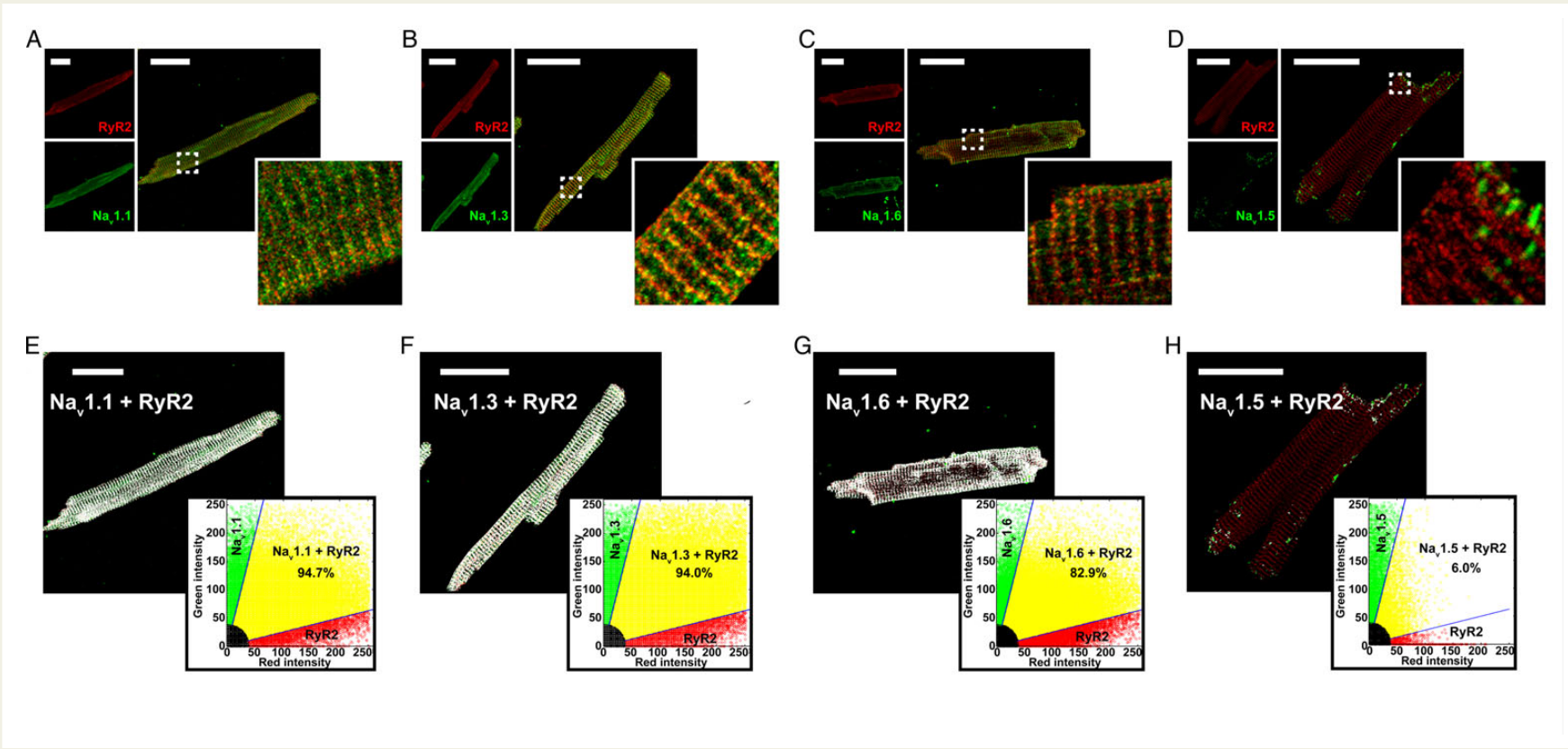

Figure 4 Neuronal Na^+ channels and RyR2 colocalize to the same discrete subcellular regions. Confocal micrographs of myocytes from R33Q mutant mice with red labelling for RyR2s (top left) and green labelling (bottom left) for (*A*) $Na_v1.1$, (*B*) $Na_v1.3$, (*C*) $Na_v1.6$, and (*D*) $Na_v1.5$ and the overlay of the two signals (right). Scale bars represent 30 μm. The dashed white box marks the region displayed in high magnification in the insets. Results of colocalization analysis for RyR2 (red) and (*E*) $Na_v1.1$, (*F*) $Na_v1.3$, (*G*) $Na_v1.6$, and (*H*) $Na_v1.5$. Images show colocalizing pixels in white, pixels with only RyR2 signal in red, and only $Na_v1.x$ signal in green. Inset plots show green ($Na_v1.x$) signal intensity plotted against red (RyR2) signal intensity. Pixels with colocalizing signals are marked in yellow, only red signal in red, only green signal in green, and weak signal intensity (background fluorescence) in black.

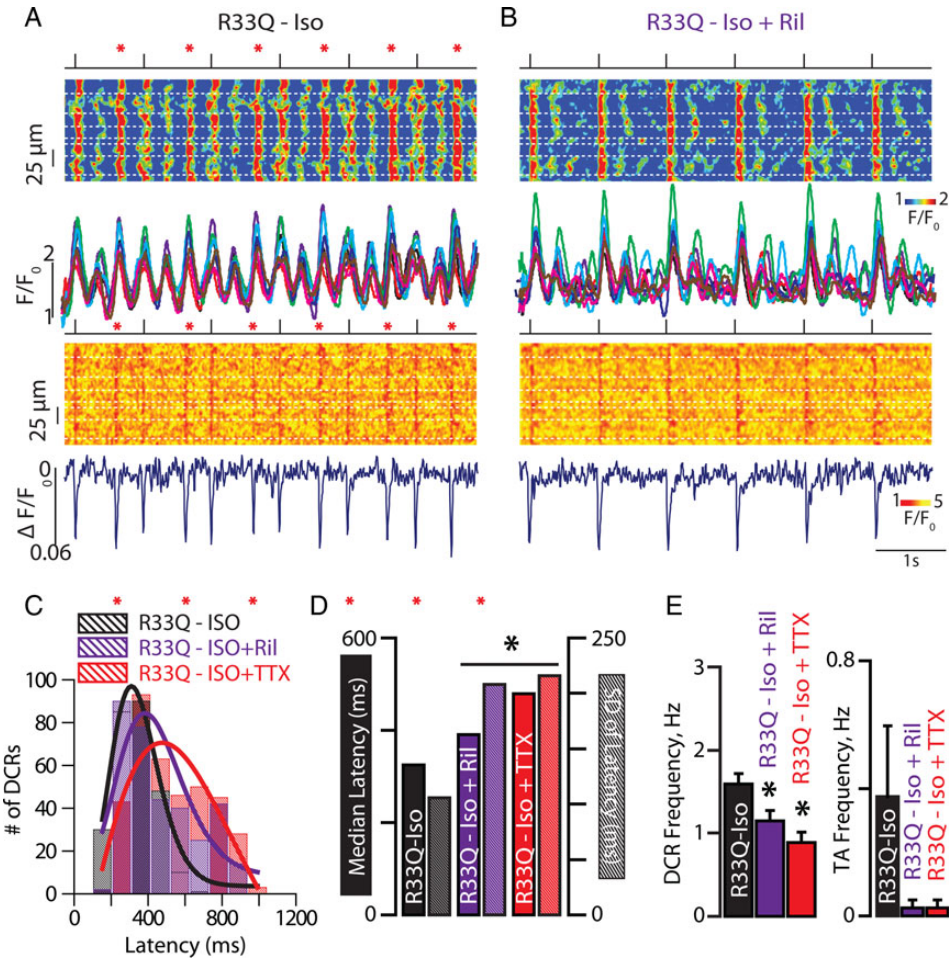

Figure 5 Neuronal Na^+ channel blockade desynchronizes DCR in tissue. Representative Ca^{2+} (top) and voltage (bottom) line-scan images of Iso-treated R33Q muscle preparations paced at 1 Hz before (*A*) and after (*B*) exposure to riluzole (Ril, 10 µM), along with the corresponding Rhod-2 fluorescence profiles from each myocyte and average di-4-ANBDQBS signal. Dashed white lines outline myocyte borders. Red asterisks indicate tissue-wide extrasystolic Ca^{2+} release (DCR) that resulted in triggered activity (TA). (*C*) Temporal distribution of DCR in cardiac muscles ($n = 264$ events for Iso alone, $n = 355$ for Ril and $n = 372$ for 100 nM TTX). (*D*) Median latencies to first DCR (solid bars) and their S.D. (hashed bars) were increased by Ril ($n = 355$ events) and TTX ($n = 372$ events) relative to Iso alone ($n = 264$ events). (*E*) DCRs and TA frequency per second (Hz) before and after treatment with Ril (10 µM; $n = 26$ cells from four preparations isolated from three mice, $^*P < 0.05$) or TTX (100 nM; $n = 29$ cells from three preparations isolated from three mice, $^*P < 0.05$).

process. Future studies will need to address the involvement of this particular subpopulation of Na^+ channels in aberrant Ca^{2+} handling.

The concept of Na^+/Ca^{2+} signalling in the vicinity of RyR2 that our data suggest is supported by previous observations that, reverse mode NCX (Na^+-out/Ca^{2+}-in) activated by the TTX-sensitive inward Na^+ current early during the action potential, can contribute to stimulated Ca^{2+} release.[17,44–47] These studies demonstrated that, during a normal heart beat, Na^+ channels modulate the efficiency of Ca^{2+} release by supplying the necessary Na^+ for reverse NCX, which in turn can facilitate RyR2 function (i.e. priming RyR2). The present study extends this concept to elucidate the mechanism of Ca^{2+}-dependent arrhythmias by providing the first evidence that the crosstalk between nNa_v along with NCX and RyR2 is critical to aberrant DCR and triggered activity. Specifically, it has been previously demonstrated that nNa_v inactivate at relatively high potentials[48] and carry a substantial residual Na^+ current during depolarization.[24] nNa_v have also been shown to exhibit substantial activity at negative membrane potentials,[25] where they are prone to activation and do not completely inactivate.[48] Thus, nNa_v activity in both stimulated and quiescent cardiomyocytes could account for the nNa_v-dependent effects observed herein. Our results further suggest that Na^+ influx through the not fully inactivated nNa_v (*Figure 2D*)[24] in the wake of electrical stimuli (*Figures 1D–F* and *3D–F*) or those that open at rest (*Figures 1A–C* and *3A–C*) may facilitate DCR by enhancing NCX-dependent Ca^{2+} accumulation in the space between the sarcolemma and the RyR2. This microdomain Ca^{2+} accumulation in turn promotes Ca^{2+}-induced Ca^{2+} release via RyR2 that are sensitized due to the presence of a pathogenic mutation in CASQ2 (*Figures 1*, *3*, and *6F*).[7–10] While a direct measurement of microdomaine Na^+ and Ca^{2+} flux in a physiologically relevant setting might be presently not feasible, our functional and structural assays targeting the key components of the Na^+/Ca^{2+} signalling provide strong evidence for its role in CPVT-associated arrhythmogenesis. Importantly, they reveal Na^+/Ca^{2+} signalling and in particular nNa_v as a therapeutic target. Future studies will have to, however, address the specific subtypes of nNa_v involved in this pro-arrhythmic process.

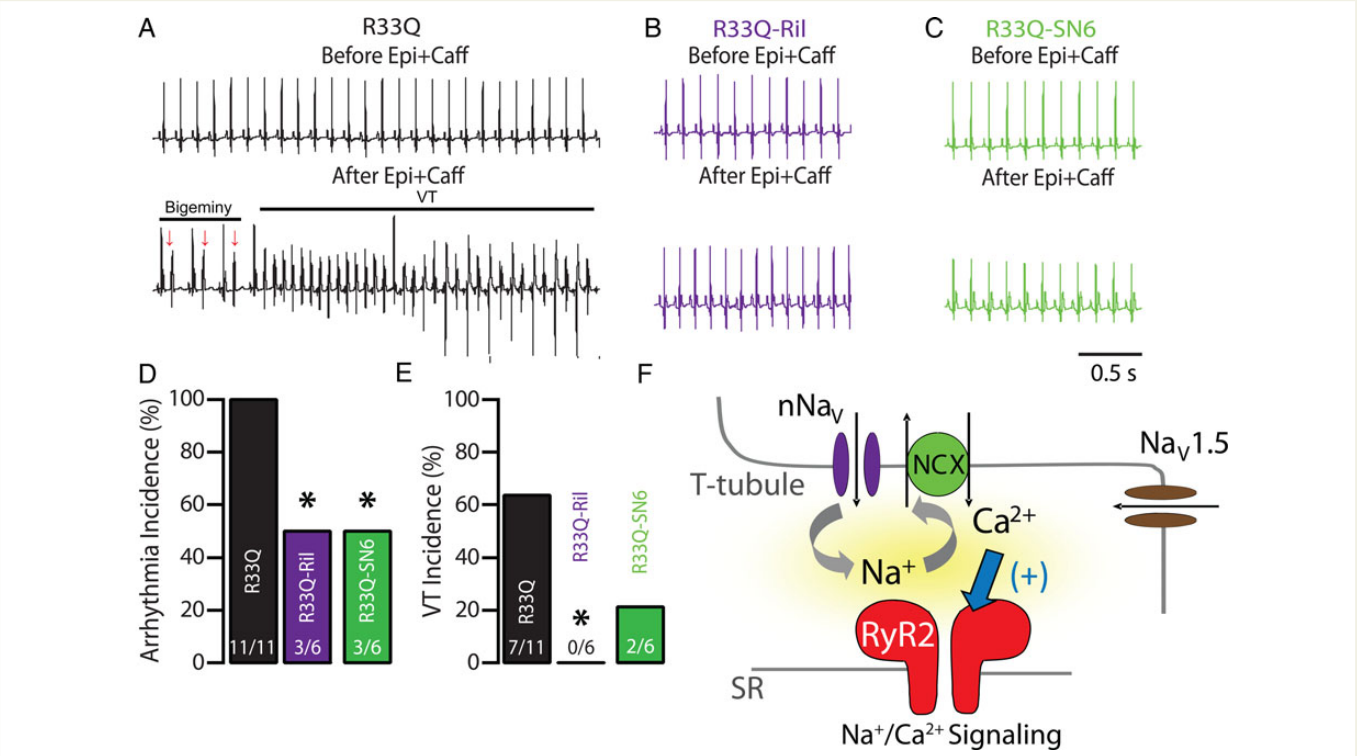

Figure 6 Effect of neuronal Na^+ channel blockade on CPVT. (*A*) Representative ECG recordings of R33Q mutant mice before (top) and after (bottom) injection (i.p.) of epinephrine (Epi, 1.5 mg/kg) and caffeine (Caff, 120 mg/kg). As illustrated in the ECG trace, Epi + Caff challenge resulted in numerous repetitive ventricular extrasystoles (arrows), bigeminy, and the induction of ventricular tachycardia (VT). (*B*) ECG of R33Q mice after administration of Ril (10 mg/kg), targeting plasma concentrations comparable to those achieved in experiments conducted in isolated cardiomyocytes,[34] before (top) and after (bottom) Epi + Caff challenge. (*C*) ECG of SN-6 (40 mg/kg) treated mice 10 min before (top) and after (bottom) Epi + Caff challenge. (*D*) Arrhythmia and (*E*) ventricular tachycardia (VT) incidence (%) in R33Q mice exposed to Epi + Caff during various interventions ($n = 6–11$ mice, $^*P < 0.05$). (*F*) Na^+/Ca^{2+} signalling: colocalization to the same discrete subcellular region allows crosstalk between neuronal Na^+ channels (nNa_v) and leaky Ca^{2+} release channels (RyR2) through the NCX resulting in aberrant DCR that underlie ventricular extrasystoles, which in turn trigger VT.

An additional unanswered question that our study attempts to tackle is how DCR can occur synchronously in sufficient amount of myocytes to elicit a ventricular extrasystole within the entire myocardium. An extrasystolic trigger must provide a depolarizing current source large enough to overcome the electrical load of connected neighbouring myocytes serving as current sinks.[49] Our data suggest that in addition to facilitating arrhythmogenic DCR on the cellular level, Na^+/Ca^{2+} signalling synchronizes aberrant DCR across the myocardium which results in triggered activity in intact cardiac tissue (*Figure 5*). The latter effect enables DCR-induced depolarization to overcome the source-sink mismatch, thereby generating ventricular extrasystole.

Interestingly, over 25 years ago Na^+ channel blockade has emerged as a promising strategy in management of Ca^{2+}-mediated arrhythmias due to heart failure.[50] However, reductions of electrical excitability have proved to be pro-arrhythmic in these patients, and class Ic antiarrhythmics are contraindicated in the population with structural heart disease due to an increased risk of arrhythmic death.[51,52] Importantly, the reduction in electrical excitability in the present as well as our previous work was not observed during selective blockade of nNa_v,[19] which nonetheless proved to be antiarrhythmic. Taken together, these data suggest a novel arrhythmogenic mechanism and provide clues to its structural underpinnings. Importantly, they also form the basis for a novel mechanism-based antiarrhythmic therapy utilizing a clinically available nNa_v blocker without compromising electrical excitability, thus causing pro-arrhythmic responses.[19,51]

Supplementary material

Supplementary material is available at *Cardiovascular Research* online.

Acknowledgements

We thank Dr Robert Gourdie for his generous assistance with preparation of confocal micrographs of immunolabeled cardiomyocytes.

Conflict of interest: none declared.

Funding

This work was supported by National Institutes of Health (NIH) Grants (HL074045, HL063043) to S.G., (HL098039-03) to P.B.R. and (HL084583, HL083422, HL114383) to P.J.M.; and ACCP Cardiology PRN Investigator Development Research Award to P.B.R.

References

1. Kong MH, Fonarow GC, Peterson ED, Curtis AB, Hernandez AF, Sanders GD, Thomas KL, Hayes DL, Al-Khatib SM. Systematic review of the incidence of sudden cardiac death in the United States. *J Am Coll Cardiol* 2011;**57**:794–801.
2. Pogwizd SM, McKenzie JP, Cain ME. Mechanisms underlying spontaneous and induced ventricular arrhythmias in patients with idiopathic dilated cardiomyopathy. *Circulation* 1998;**98**:2404–2414.
3. Leenhardt A, Lucet V, Denjoy I, Grau F, Ngoc DD, Coumel P. Catecholaminergic polymorphic ventricular tachycardia in children. A 7-year follow-up of 21 patients. *Circulation* 1995;**91**:1512–1519.

4. Marks AR, Priori S, Memmi M, Kontula K, Laitinen PJ. Involvement of the cardiac ryanodine receptor/calcium release channel in catecholaminergic polymorphic ventricular tachycardia. *J Cell Physiol* 2002;**190**:1–6.
5. Knollmann BC, Chopra N, Hlaing T, Akin B, Yang T, Ettensohn K, Knollmann BEC, Horton KD, Weissman NJ, Holinstat I, Zhang W, Roden DM, Jones LR, Franzini-Armstrong C, Pfeifer K. Casq2 deletion causes sarcoplasmic reticulum volume increase, premature Ca2+ release, and catecholaminergic polymorphic ventricular tachycardia. *J Clin Invest* 2006;**116**:2510–2520.
6. Priori SG, Napolitano C, Tiso N, Memmi M, Vignati G, Bloise R, Sorrentino V, Danieli GA. Mutations in the cardiac ryanodine receptor gene (hRyR2) underlie catecholaminergic polymorphic ventricular tachycardia. *Circulation* 2001;**103**:196–200.
7. Kornyeyev D, Petrosky AD, Zepeda B, Ferreiro M, Knollmann B, Escobar AL. Calsequestrin 2 deletion shortens the refractoriness of Ca^{2+} release and reduces rate-dependent Ca^{2+}-alternans in intact mouse hearts. *J Mol Cell Cardiol* 2012;**52**:21–31.
8. Brunello L, Slabaugh JL, Radwanski PB, Ho H-T, Belevych AE, Lou Q, Chen H, Napolitano C, Lodola F, Priori SG, Fedorov VV, Volpe P, Fill M, Janssen PML, Györke S. Decreased RyR2 refractoriness determines myocardial synchronization of aberrant Ca2+ release in a genetic model of arrhythmia. *Proc Natl Acad Sci USA* 2013;**110**:10312–10317.
9. Loaiza R, Benkusky NA, Powers PP, Hacker T, Noujaim S, Ackerman MJ, Jalife J, Valdivia HH. Heterogeneity of ryanodine receptor dysfunction in a mouse model of catecholaminergic polymorphic ventricular tachycardia. *Circ Res* 2013;**112**:298–308.
10. Belevych AE, Terentyev D, Terentyeva R, Ho H-T, Gyorke I, Bonilla IM, Carnes CA, Billman GE, Györke S. Shortened Ca2+ signaling refractoriness underlies cellular arrhythmogenesis in a postinfarction model of sudden cardiac death. *Circ Res* 2012;**110**:569–577.
11. Radwański PB, Belevych AE, Brunello L, Carnes CA, Györke S. Store-dependent deactivation: cooling the chain-reaction of myocardial calcium signaling. *J Mol Cell Cardiol* 2013;**58**:77–83.
12. ter Keurs HEDJ, Boyden PA. Calcium and arrhythmogenesis. *Physiol Rev* 2007;**87**:457–506.
13. Knollmann BC. Power and pitfalls of using transgenic mice to optimize therapy for CPVT – a need for prospective placebo-controlled clinical trials in genetic arrhythmia disorders. *Heart Rhythm* 2010;**7**:1683–1685.
14. Zhu C, Barker RJ, Hunter AW, Zhang Y, Jourdan J, Gourdie RG. Quantitative analysis of ZO-1 colocalization with Cx43 gap junction plaques in cultures of rat neonatal cardiomyocytes. *Microsc Microanal* 2005;**11**:244–248.
15. Rizzi N, Liu N, Napolitano C, Nori A, Turcato F, Colombi B, Bicciato S, Arcelli D, Spedito A, Scelsi M, Villani L, Esposito G, Boncompagni S, Protasi F, Volpe P, Priori SG. Unexpected structural and functional consequences of the R33Q homozygous mutation in cardiac calsequestrin: a complex arrhythmogenic cascade in a knock in mouse model. *Circ Res* 2008;**103**:298–306.
16. Liu N, Denegri M, Dun W, Boncompagni S, Lodola F, Protasi F, Napolitano C, Boyden PA, Priori SG. Abnormal propagation of calcium waves and ultrastructural remodeling in recessive catecholaminergic polymorphic ventricular tachycardia. *Circ Res* 2013;**113**:142–152.
17. Torres NS, Larbig R, Rock A, Goldhaber JI, Bridge JHB. Na+ currents are required for efficient excitation-contraction coupling in rabbit ventricular myocytes: a possible contribution of neuronal Na+ channels. *J Physiol* 2010;**588**:4249–4260.
18. Hwang HS, Hasdemir C, Laver D, Mehra D, Turhan K, Faggioni M, Yin H, Knollmann BC. Inhibition of cardiac Ca2+ release channels (RyR2) determines efficacy of class I antiarrhythmic drugs in catecholaminergic polymorphic ventricular tachycardia. *Circ Arrhythm Electrophysiol* 2011;**4**:128–135.
19. Radwański PB, Greer-Short A, Poelzing S. Inhibition of Na+ channels ameliorates arrhythmias in a drug-induced model of Andersen-Tawil syndrome. *Heart Rhythm* 2013;**10**:255–263.
20. Buchanan JW Jr, Saito T, Gettes LS. The effects of antiarrhythmic drugs, stimulation frequency, and potassium-induced resting membrane potential changes on conduction velocity and dV/dtmax in guinea pig myocardium. *Circ Res* 1985;**56**:696–703.
21. Sikkel MB, Collins TP, Rowlands C, Shah M, O'Gara P, Williams AJ, Harding SE, Lyon AR, MacLeod KT. Flecainide reduces Ca(2+) spark and wave frequency via inhibition of the sarcolemmal sodium current. *Cardiovasc Res* 2013;**98**:286–296.
22. Song JH, Huang CS, Nagata K, Yeh JZ, Narahashi T. Differential action of riluzole on tetrodotoxin-sensitive and tetrodotoxin-resistant sodium channels. *J Pharmacol Exp Ther* 1997;**282**:707–714.
23. Bensimon G, Lacomblez L, Meininger V. A controlled trial of riluzole in amyotrophic lateral sclerosis. ALS/Riluzole Study Group. *N Engl J Med* 1994;**330**:585–591.
24. Conforti L, Tohse N, Sperelakis N. Tetrodotoxin-sensitive sodium current in rat fetal ventricular myocytes--contribution to the plateau phase of action potential. *J Mol Cell Cardiol* 1993;**25**:159–173.
25. Duclohier H. Neuronal sodium channels in ventricular heart cells are localized near T-tubules openings. *Biochem Biophys Res Commun* 2005;**334**:1135–1140.
26. Schiavon E, Stevens M, Zaharenko AJ, Konno K, Tytgat J, Wanke E. Voltage-gated sodium channel isoform-specific effects of pompilidotoxins. *FEBS J* 2010;**277**:918–930.
27. Niu C-F, Watanabe Y, Ono K, Iwamoto T, Yamashita K, Satoh H, Urushida T, Hayashi H, Kimura J. Characterization of SN-6, a novel Na+/Ca2+ exchange inhibitor in guinea pig cardiac ventricular myocytes. *Eur J Pharmacol* 2007;**573**:161–169.
28. Iwamoto T, Inoue Y, Ito K, Sakaue T, Kita S, Katsuragi T. The exchanger inhibitory peptide region-dependent inhibition of Na+/Ca2+ exchange by SN-6 [2-[4-(4-nitrobenzyloxy) benzyl]thiazolidine-4-carboxylic acid ethyl ester], a novel benzyloxyphenyl derivative. *Mol Pharmacol* 2004;**66**:45–55.
29. Neco P, Rose B, Huynh N, Zhang R, Bridge JHB, Philipson KD, Goldhaber JI. Sodium-calcium exchange is essential for effective triggering of calcium release in mouse heart. *Biophys J* 2010;**99**:755–764.
30. Jayasinghe ID, Cannell MB, Soeller C. Organization of ryanodine receptors, transverse tubules, and sodium-calcium exchanger in rat myocytes. *Biophys J* 2009;**97**:2664–2673.
31. Maier SKG, Westenbroek RE, McCormick KA, Curtis R, Scheuer T, Catterall WA. Distinct subcellular localization of different sodium channel alpha and beta subunits in single ventricular myocytes from mouse heart. *Circulation* 2004;**109**:1421–1427.
32. Maltsev AV, Maltsev VA, Mikheev M, Maltseva LA, Sirenko SG, Lakatta EG, Stern MD. Synchronization of stochastic $Ca^2(+)$ release units creates a rhythmic $Ca^2(+)$ clock in cardiac pacemaker cells. *Biophys J* 2011;**100**:271–283.
33. Stern MD, Kort AA, Bhatnagar GM, Lakatta EG. Scattered-light intensity fluctuations in diastolic rat cardiac muscle caused by spontaneous Ca++-dependent cellular mechanical oscillations. *J Gen Physiol* 1983;**82**:119–153.
34. Milane A, Tortolano L, Fernandez C, Bensimon G, Meininger V, Farinotti R. Brain and plasma riluzole pharmacokinetics: effect of minocycline combination. *J Pharm Pharm Sci* 2009;**12**:209–217.
35. Terentyev D, Nori A, Santoro M, Viatchenko-Karpinski S, Kubalova Z, Gyorke I, Terentyeva R, Vedamoorthyrao S, Blom NA, Valle G, Napolitano C, Williams SC, Volpe P, Priori SG, Gyorke S. Abnormal interactions of calsequestrin with the ryanodine receptor calcium release channel complex linked to exercise-induced sudden cardiac death. *Circ Res* 2006;**98**:1151–1158.
36. Terentyev D, Viatchenko-Karpinski S, Györke I, Volpe P, Williams SC, Györke S. Calsequestrin determines the functional size and stability of cardiac intracellular calcium stores: Mechanism for hereditary arrhythmia. *Proc Natl Acad Sci USA* 2003;**100**:11759–11764.
37. Watanabe H, Chopra N, Laver D, Hwang HS, Davies SS, Roach DE, Duff HJ, Roden DM, Wilde AAM, Knollmann BC. Flecainide prevents catecholaminergic polymorphic ventricular tachycardia in mice and humans. *Nat Med* 2009;**15**:380–383.
38. Liu N, Denegri M, Ruan Y, Avelino-Cruz JE, Perissi A, Negri S, Napolitano C, Coetzee WA, Boyden PA, Priori SG. Short communication: flecainide exerts an antiarrhythmic effect in a mouse model of catecholaminergic polymorphic ventricular tachycardia by increasing the threshold for triggered activity. *Circ Res* 2011;**109**:291–295.
39. Weiss S, Benoist D, White E, Teng W, Saint DA. Riluzole protects against cardiac ischaemia and reperfusion damage via block of the persistent sodium current. *Br J Pharmacol* 2010;**160**:1072–1082.
40. Maier SKG, Westenbroek RE, Schenkman KA, Feigl EO, Scheuer T, Catterall WA. An unexpected role for brain-type sodium channels in coupling of cell surface depolarization to contraction in the heart. *Proc Natl Acad Sci USA* 2002;**99**:4073–4078.
41. Westenbroek RE, Bischoff S, Fu Y, Maier SKG, Catterall WA, Scheuer T. Localization of sodium channel subtypes in mouse ventricular myocytes using quantitative immunocytochemistry. *J Mol Cell Cardiol* 2013;**64**:69–78.
42. Lin X, Liu N, Lu J, Zhang J, Anumonwo JMB, Isom LL, Fishman GI, Delmar M. Subcellular heterogeneity of sodium current properties in adult cardiac ventricular myocytes. *Heart Rhythm* 2011;**8**:1923–1930.
43. Lin X, O'Malley H, Chen C, Auerbach D, Foster M, Shekhar A, Zhang M, Coetzee W, Jalife J, Fishman GI, Isom L, Delmar M. Scn1b deletion leads to increased tetrodotoxin-sensitive sodium current, altered intracellular calcium homeostasis and arrhythmias in murine hearts. *J Physiol* 2014; doi:10.1113/jphysiol.2014.277699.
44. Larbig R, Torres N, Bridge JHB, Goldhaber JI, Philipson KD. Activation of reverse Na+-Ca2+ exchange by the Na+ current augments the cardiac Ca2+ transient: evidence from NCX knockout mice. *J Physiol* 2010;**588**:3267–3276.
45. Lipp P, Niggli E. Sodium current-induced calcium signals in isolated guinea-pig ventricular myocytes. *J Physiol* 1994;**474**:439–446.
46. Sipido KR, Carmeliet E, Pappano A. Na+ current and Ca2+ release from the sarcoplasmic reticulum during action potentials in guinea-pig ventricular myocytes. *J Physiol* 1995;**489**:1–17.
47. Murphy E, Eisner DA. Regulation of intracellular and mitochondrial sodium in health and disease. *Circ Res* 2009;**104**:292–303.
48. Ulbricht W. Sodium channel inactivation: molecular determinants and modulation. *Physiol Rev* 2005;**85**:1271–1301.
49. Xie Y, Sato D, Garfinkel A, Qu Z, Weiss JN. So little source, so much sink: requirements for afterdepolarizations to propagate in tissue. *Biophys J* 2010;**99**:1408–1415.
50. The Cardiac Arrhythmia Pilot Study. The CAPS investigators. *Am J Cardiol* 1986;**57**:91–95.
51. Starmer CF, Lastra AA, Nesterenko VV, Grant AO. Proarrhythmic response to sodium channel blockade. Theoretical model and numerical experiments. *Circulation* 1991;**84**:1364–1377.
52. Echt DS, Liebson PR, Mitchell LB, Peters RW, Obias-Manno D, Barker AH, Arensberg D, Baker A, Friedman L, Greene HL. Mortality and morbidity in patients receiving encainide, flecainide, or placebo. The Cardiac Arrhythmia Suppression Trial. *N Engl J Med* 1991;**324**:781–788.